PHYSICAL REVIEW C

NUCLEAR PHYSICS

THIRD SERIES, VOLUME 52, NUMBER 6 | DECEMBER 1995

RAPID COMMUNICATIONS

The Rapid Communications section is intended for the accelerated publication of important new results. Manuscripts submitted to this section are given priority in handling in the editorial office and in production. A Rapid Communication in **Physical Review C** *may be no longer than five printed pages and must be accompanied by an abstract. Page proofs are sent to authors.*

Low energy resonances in $^{15}N(\alpha,\gamma)^{19}F$ and $^{15}O(\alpha,\gamma)^{19}Ne$

S. Wilmes, P. Mohr, U. Atzrott, V. Kölle, and G. Staudt

Physikalisches Institut, Universität Tübingen, D–72076 Tübingen, Germany

A. Mayer and J. W. Hammer

Institut für Strahlenphysik, Universität Stuttgart, D–70569 Stuttgart, Germany

(Received 7 August 1995)

The $E_{\alpha,\mathrm{lab}}=679$ keV $(\frac{5}{2}^+)$ and $E_{\alpha,\mathrm{lab}}=687$ keV $(\frac{3}{2}^-)$ resonances in the $^{15}N(\alpha,\gamma)^{19}F$ reaction have been analyzed using a windowless gas target system and a 100% relative efficiency germanium detector with an active BGO shielding. The strength of the $E_{\alpha,\mathrm{lab}}=687$ keV resonance has been determined: $\omega\gamma= 8\pm3$ μeV. The strength of the $E_{\alpha,\mathrm{lab}}=461$ keV resonance and the properties of the corresponding resonances in the mirror reaction $^{15}O(\alpha,\gamma)^{19}Ne$ have been derived using a realistic folding potential.

PACS number(s): 25.55.−e, 24.30.Gd, 95.30.Cq

A possible scenario for the production of fluorine is the nucleosynthesis in so-called AGB stars during thermal pulses. The chain $^{14}N(\alpha,\gamma)^{18}F(\beta^+)^{18}O(p,\alpha)^{15}N(\alpha,\gamma)^{19}F$ seems to be responsible for the production of ^{19}F. Even if there are some contributions from other reaction chains, they all have in common that the reaction $^{15}N(\alpha,\gamma)^{19}F$ is the last step for the synthesis of fluorine [1,2].

The reaction $^{15}O(\alpha,\gamma)^{19}Ne$ is of special interest for the escape from the hot CNO cycle (HCNO). The HCNO cycle takes place when the proton capture by ^{13}N is faster than the β decay of this nucleus and the rate of converting H to He is limited by the β decay of ^{14}O and ^{15}O. At temperatures high enough the α capture by ^{15}O is equal to or even greater than the β decay and a breakout from the HCNO is possible through $^{15}O(\alpha,\gamma)^{19}Ne(p,\gamma)^{20}Na$ [3,4]. At temperatures where a significant conversion of ^{15}O to ^{19}Ne takes place, the proton capture by ^{19}Ne is dominant in comparison to the β decay of ^{19}Ne. Therefore the reaction $^{15}O(\alpha,\gamma)^{19}Ne$ limits the outflow from the HCNO [4]. At the moment this reaction cannot be measured directly, but information can be obtained by measuring the mirror reaction $^{15}N(\alpha,\gamma)^{19}F$.

Up to now the reaction $^{15}N(\alpha,\gamma)^{19}F$ was studied in several experiments [5–9]. In the most interesting low energy region recently an experiment was performed by Magnus *et al.* [10]. It was carried out using a thick $Ti^{15}N$ target and a 35% Ge(Li) detector in close geometry. Two levels were analyzed at $E_{\alpha,\mathrm{lab}}=679$ keV ($E_x=4550$ keV, $\frac{5}{2}^+$) and $E_{\alpha,\mathrm{lab}}=687$ keV ($E_x=4556$ keV, $\frac{3}{2}^-$), respectively. For the $\frac{5}{2}^+$ state they found a resonance strength of $\omega\gamma=(97\pm20)$ μeV whereas for the $\frac{3}{2}^-$ state only an upper limit of $\omega\gamma< 10$ μeV was stated.

Now we have measured the reaction $^{15}N(\alpha,\gamma)^{19}F$ in the energy range 650 keV $<E_{\alpha,\mathrm{lab}}<$2650 keV. The data obtained at higher energies will be published later, and we present our results in the low energy range only. It was the aim of this part of the experiment to measure the resonance strength of the 4556 keV $(\frac{3}{2}^-)$ resonance and to extend the results to the mirror reaction $^{15}O(\alpha,\gamma)^{19}Ne$. The setup of our experiment was similar to that described in [11]: We used the windowless gas target facility RHINOCEROS with a 99% enriched $^{15}N_2$ gas, a pressure of 1.2 mbar, and an effective target length of about 6 cm. The α-beam current from the Dynamitron accelerator of the IFS Stuttgart was about 80 μA. The elastically scattered α particles were measured with two surface barrier detectors to normalize the yield of the γ rays.

For the detection of the γ quanta a high-purity germanium detector (HPGe) with a relative efficiency of about 100% was used. The detector was arranged in close geometry perpendicular to the beam axis and symmetrical to the target chamber covering γ-ray angles from 60° to 120°. The distance to the beam of about 8 cm was as small as possible. For background reduction the HPGe detector was surrounded by an active BGO shield. Both detectors were embedded in a lead block serving as passive background shield. The BGO detector is made up of eight segments, each segment having its own photomultiplier [12]. The eight outputs build a stop signal for a time-to-amplitude converter (TAC), whereas the start signal is generated via the timing output of the HPGe detector. The achieved time resolution is better than 15 ns (FWHM). All signals from the TAC output within a 60 ns window around the peak maximum are defined as coincident. They are selected with a SCA and give an anticoincidence gate for the HPGe output. In this way all events giving simultaneously an output from at least one segment of the BGO and from the HPGe detector are rejected. The application of the BGO shield leads to a reduction of the background by a factor of 8 in the relevant energy region (Fig. 1).

The dominant peak in these spectra represents the transition $R(4550) \rightarrow 197$. The total widths of both the 4550 and 4556 keV resonances are small compared with the energy loss of the α particles in the target gas ($\Delta E_{\mathrm{c.m.}} = 14$ keV) [13]. Therefore in this "thick target experiment" the position of the resonant interaction within the chamber is fixed by the incident energy. Due to the small energy difference of 6 keV both resonances can be excited simultaneously in the target chamber. The position of the dominant resonance $R(4550) \rightarrow 197$ can be obtained from the measured yield (Fig. 2, left-hand side) and is confirmed by the Doppler shift of the energy of the emitted γ quanta (Fig. 2, right-hand side). It results that at $E_{\alpha,\mathrm{lab}} = 670$ keV the 4550 keV resonant interaction is located in the vicinity of the entrance slit of the target chamber while at $E_{\alpha,\mathrm{lab}} = 688$ keV it is located at the exit slit. In the first case the beam energy is too low to excite the 4556 keV resonance, whereas in the second case this resonance is located in the center of the target chamber.

At these two energies long time runs (≈ 50 h) have been performed. The results are shown in Fig. 3. In both spectra the transition $R(4550) \rightarrow 197$ (branching ratio 69% [14]) is dominating. Comparing the spectra the Doppler shift to lower energies with increasing beam energy can clearly be observed. The bump indicated in the lower spectrum represents the transition $R(4556) \rightarrow 110$ (branching ratio 45% [14]). After normalization with respect to the measured yield curve and the branching ratios one can determine the

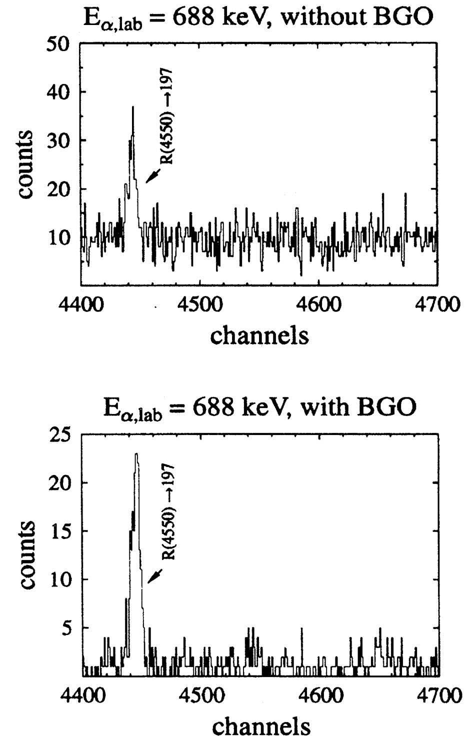

FIG. 1. Spectra of the reaction $^{15}N(\alpha,\gamma)\,^{19}F$ measured simultaneously with and without active BGO shielding. In the lower part the BGO gate was used whereas in the upper part no anticoincidence signal was applied. The relevant transition energy for $R(4550) \rightarrow 197$ is marked by an arrow.

strength of the 4556 keV resonance in comparison to the 4550 keV resonance. Using $\omega\gamma(4550) = (97 \pm 20)$ μeV [10] one obtains $\omega\gamma(4556) = (8 \pm 3)$ μeV. This result agrees well with the upper limit given by Magnus *et al.* [10]: $\omega\gamma < 10$ μeV.

For both resonances the α energy is small compared with the energy of the Coulomb barrier; therefore, $\Gamma_\alpha \ll \Gamma_\gamma$ can be assumed. Then the α width of both states can easily be deduced as listed in Table I. There are two possibilities to extract (model-dependent) values for the reduced width θ_α^2. First, θ_α^2 can be calculated using the Wigner limit (with a

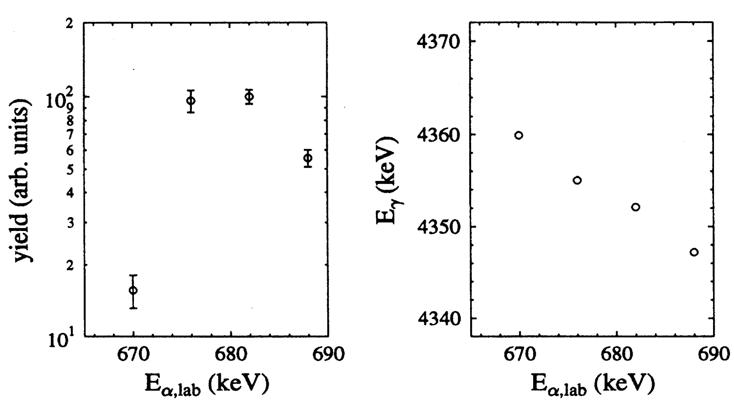

FIG. 2. On the left-hand side the yield curve of the transition $R(4550) \rightarrow 197$, on the right-hand side the energy shift of the γ rays due to the Doppler effect is shown. The α energies are related to the center of the target chamber. Both curves together give information about the position of the 4550 keV resonance within the target chamber.

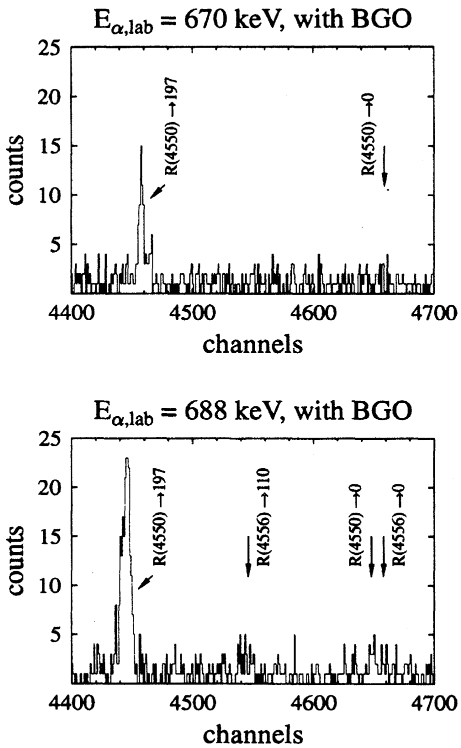

FIG. 3. Spectra of the reaction ^{15}N(α,γ)^{19}F measured at $E_{\alpha,\rm lab}$ = 670 keV and $E_{\alpha,\rm lab}$ = 688 keV. These energies are related to the position of the 4550 keV resonance in the entrance and the exit slits of the target chamber, respectively. The relevant transition energies are marked by arrows.

channel radius $R_N=6.0$ fm). Second, the scattering phase shifts δ_{LJ} and subsequently the resonance widths $\Gamma_\alpha=2\times[(d\delta_{LJ}/dE)|_{E=E_{\rm res}}]^{-1}$ can be calculated using a proper ^{15}N-α potential the depth of which is adjusted in order to match the energies of the levels concerned. Then using $\Gamma_\alpha^{\rm exp}=\Gamma_\alpha^{\rm cal}\times\theta^2_{\alpha,\rm pot}$ one obtains the values given in the last column of Table I. In our potential model calculation we use a ^{15}N-α potential deduced by a double-folding procedure [15] and wave functions with three nodes ($\frac{3}{2}^-$, $L=2$) and 2 nodes ($\frac{5}{2}^+$ and $\frac{7}{2}^+$, $L=3$).

There is a further resonance in ^{19}F at 4378 keV ($\frac{7}{2}^+$) which is of astrophysical interest. The resonance strength of this state given in the third line of Table I cannot be measured directly with the existing experimental setup. But it can be calculated by assuming $\theta^2_\alpha(4378)\approx\theta^2_\alpha(4550)$. Both states are members of the same ($K^\pi=\frac{3}{2}^+$) band and exhibit the same (^{12}C$\otimes$^{7}Li) cluster structure [16]. Using either $\theta^2_{\alpha,\rm WL}$ or $\theta^2_{\alpha,\rm pot}$ we obtain in both model calculations nearly the same α width Γ_α=0.024 μeV and subsequently nearly the same value for the resonance strength of $\omega\gamma(4378)\approx0.1$ μeV. This result is a factor of 16 higher than a value which was recently extracted from an analysis of the transfer reaction ^{15}N(^{7}Li,t)^{19}F: $\Gamma_\alpha=1.5\times10^{-9}$ eV [17]. But such a small value for $\Gamma_\alpha(4378)$ is in contradiction to different analyses of the mirror nucleus ^{19}Ne (see below).

In order to calculate the resonance strengths for the analogous states in the mirror nucleus ^{19}Ne we assume the equality of the reduced widths θ^2_α of the analogous states in ^{19}F and ^{19}Ne. With this assumption we have calculated the α widths given in Table II. Due to the lower α threshold in ^{19}Ne compared to ^{19}F, the α widths of the ^{19}Ne states are found to be about three orders of magnitude larger than those in ^{19}F. It should be pointed out again that both methods to determine Γ_α result in very similar values though the reduced widths $\theta^2_{\alpha,\rm pot}$ obtained in the potential model calculation are quite different from those values $\theta^2_{\alpha,\rm WL}$ obtained in the calculation using the Wigner limit $\gamma^2_{\rm WL}$.

In contrast to ^{19}F the approximation $\Gamma_\alpha\ll\Gamma_\gamma$ and thereby the relation $\gamma=\Gamma_\alpha$ is no longer valid for ^{19}Ne states. But the γ widths Γ_γ and subsequently both the total width Γ and the resonance strengths $\omega\gamma$ can be obtained for all resonances by combining the calculated α widths Γ_α with the Γ_α/Γ data recently extracted in a study of the reaction ^{19}F(^{3}He,t)^{19}Ne* [18]. The results are given in Table II together with the values of the resonance strengths given by Magnus *et al.* [18]. In order to calculate the strength of the $\frac{5}{2}^+$ resonance we applied the same method as used by Magnus *et al.*; of course the results agree well. For the $\frac{3}{2}^-$ resonance Magnus *et al.* had to combine their measured branching Γ_α/Γ with the upper limit of Γ_α [10] and the lower limit of Γ_γ [14] in ^{19}F. Our result which is based on the experimental Γ_α value of the mirror state in ^{19}F is somewhat larger but agrees within the relatively large uncertainties. For the $\frac{7}{2}^+$ resonance Magnus *et al.* [18] can only state a lower limit from the combination of their measured branching Γ_α/Γ and the lower limit of Γ_γ of the mirror state in ^{19}F [14]. Assuming $\theta^2_\alpha(\frac{7}{2}^+)=\theta^2_\alpha(\frac{5}{2}^+)$ our result is about 10% larger than the lower limit given in [18]. Therefore, our assumption is confirmed by the result of Magnus *et al.*, but there is a clear contradiction to the recent analysis of the reaction ^{15}N(^{7}Li,t)^{19}F [17].

TABLE I. Resonance parameters of ^{19}F.

J^π (K^π)	E_x (keV)	$E_{\rm c.m.}$ (keV)	$\omega\gamma$ (μeV)	Γ_α (μeV)	$\theta^2_{\alpha,\rm WL}$ [a]	$\theta^2_{\alpha,\rm pot}$ [b]
$\frac{3}{2}^-$(-)	4556	542	8±3	4	0.0002	0.00077
$\frac{5}{2}^+$ ($\frac{3}{2}^+$)	4550	536	97±20[c]	32.3	0.0172	0.129
$\frac{7}{2}^+$ ($\frac{3}{2}^+$)	4378	364	≈0.1	0.024	0.0172[d]	0.129[d]

[a]Derived from Wigner limit.
[b]Deduced from potential model calculation.
[c]Reference [10].
[d]$\theta^2_\alpha(4378)=\theta^2_\alpha(4550)$ assumed.

TABLE II. Resonance parameters of ^{19}Ne.

J^π (K^π)	E_x (keV)	$E_{c.m.}$ (keV)	$\Gamma_{\alpha,WL}$ [a] (meV)	$\Gamma_{\alpha,pot}$ [b] (meV)	Γ_γ (meV)	Γ (meV)	$\omega\gamma$ [b] (meV)	$\omega\gamma$ [c] (meV)
$\frac{3}{2}^-$(-)	4549	1020	3.2	3.4	45	48.4	6.3	4.5±2.5
$\frac{5}{2}^+$ ($\frac{3}{2}^+$)	4600	1071	81.9	83	250	333	187	198±51
$\frac{7}{2}^+$ ($\frac{3}{2}^+$)	4379	850	3.0	2.9	62	64.9	11	>10

[a]Derived from Wigner limit.
[b]Deduced from potential model calculation.
[c]Reference [18].

Finally, assuming the same γ widths for the analogous states in ^{19}F the values deduced in this way can be compared with the adopted ones [14]. A good agreement between the two values is found for the 4556 keV ($\frac{3}{2}^-$) state: Γ_γ=44.8 meV vs $\Gamma_\gamma=(39^{+34}_{-15})$ meV [14,18]. For the 4378 keV ($\frac{7}{2}^+$) state the deduced value (Γ_γ=61.9 meV) is only slightly larger than the lower limit value (Γ_γ>60 meV) given in [14]. But for the 4550 keV ($\frac{5}{2}^+$) state the deduced value (Γ_γ=250 meV) is more than one order of magnitude larger than the lower limit value (Γ_γ>13 meV) listed in [14]. On the other hand, now the transition strength for the ground state transition reported in Ref. [19] but not listed in Ref. [14] can easily be incorporated. The value S (4550→0) =(1.0±0.2) W.u. [19] corresponds to a γ width Γ_{γ_0}=4.8 meV and subsequently to a branching ratio of about 2%.

In the γ spectra obtained in our experiment at incident energies between 670 keV and 688 keV (see Fig. 3) some hints can be found for this transition. Especially at $E_{\alpha,lab}$ =688 keV (lower part of Fig. 3) a broad structure is observed in the marked energy region. In this γ energy range one expects the transitions R(4550)→0 and R(4556)→0. Due to the different Doppler corrections the energy difference between the two expected peaks is larger than 6 keV. The number of events observed in this broad structure is compatible with the expected one supposing a branching ratio of 2% for the R(4550)→0 transition and of 36% for the R(4556)→0 transition. In a calculation using the code GEANT [20] the measured γ spectrum was simulated. It results that sum peak contributions can be neglected.

Concluding our results we state that the new experimental value of the resonance strength $\omega\gamma$(4556)=(8±3) μeV together with the results of our calculation confirm the reaction rates determined for both reactions ^{15}N(α,γ)^{19}F and ^{15}O(α,γ)^{19}Ne in the astrophysically relevant energy range. Beyond it new values for the γ transition strength, especially for the E_x=4550 keV ($\frac{5}{2}^+$) state in ^{19}F, have been deduced.

We would like to thank the Deutsche Forschungsgemeinschaft (DFG projects Sta290, and Graduiertenkolleg Mu705) and the Institut für Strahlenphysik der Universität Stuttgart for the support during beamtimes.

[1] A. Jorissen, V. V. Smith, and D. L. Lambert, Astron. Astrophys. **261**, 164 (1992).
[2] M. Forestini, S. Goriely, A. Jorissen, and M. Arnould, Astron. Astrophys. **261**, 157 (1992).
[3] R. K. Wallace and S. E. Woosley, Astrophys. J. Suppl. **45**, 389 (1981).
[4] K. Langanke, M. Wiescher, W. A. Fowler, and J. Görres, Astrophys. J. **301**, 629 (1986).
[5] J. H. Aitken, R. E. Azuma, A. E. Litherland, A. M. Charlesworth, D. W. O. Rogers, and J. J. Simpson, Can. J. Phys. **48**, 1617 (1970).
[6] W. R. Dixon and R. S. Storey, Can. J. Phys. **49**, 1714 (1971).
[7] D. W. Rogers, J. H. Aitken, and A. E. Litherland, Can. J. Phys. **50**, 268 (1972).
[8] D. W. O. Rogers, R. P. Beukens, and W. T. Diamond, Can. J. Phys. **50**, 2428 (1972).
[9] W. R. Dixon and R. S. Storey, Nucl. Phys. **A284**, 97 (1977).
[10] P. V. Magnus, M. S. Smith, P. D. Parker, R. E. Azuma, C. Campbell, J. D. King, and J. Vise, Nucl. Phys. **A470**, 206 (1987).
[11] P. Mohr, V. Kölle, S. Wilmes, U. Atzrott, G. Staudt, J. W. Hammer, H. Krauss, and H. Oberhummer, Phys. Rev. C **50**, 1543 (1994).
[12] H. Maser, J. Markgraf, and A. Mayer, IFS report 4/94, Univ. Stuttgart (1994) (internal report).
[13] J. F. Ziegler, *Helium Stopping Powers and Ranges in All Elements* (Pergamon, New York, 1977).
[14] F. Ajzenberg-Selove, Nucl. Phys. **A475**, 1 (1987).
[15] H. Abele and G. Staudt, Phys. Rev. C **47**, 742 (1993).
[16] P. Descouvemont and D. Baye, Nucl. Phys. **A463**, 629 (1987).
[17] F. de Oliviera, A. Coc, P. Aguer, C. Angulo, G. Bogaert, S. Fortier, J. Kiener, A. Lefebvre, J. M. Maison, L. Rosier, G. Rotbard, V. Tatischeff, J. P. Thibaud, and J. Vernotte, in *Proceedings of the Third International Symposium on Nuclear Astrophysics: Nuclei in the Cosmos*, Gran Sasso, Italy, 1994, edited by M. Busso, R. Gallino, and C. M. Raiteri, AIP Conf. Proc. No. 327 (AIP, New York, 1995), p. 311.
[18] P. V. Magnus, M. S. Smith, A. J. Howard, P. D. Parker, and A. E. Champagne, Nucl. Phys. **A506**, 332 (1990).
[19] P. M. Endt, At. Data Nucl. Data Tables **23**, 3 (1979).
[20] R. Brun and F. Carminati, GEANT Detector Description and Simulation Tool, CERN Program Library Long Writeup W5013 edition, CERN, Geneva (1993).